Dynamic contour error compensation in micro/nano machining of hardened steel by applying elliptical vibration sculpturing method

Jianguo Zhang[1,2], Norikazu Suzuki[2], Eiji Shamoto[2*], Jianfeng Xu[1*]

[1] State Key Laboratory of Digital Manufacturing Equipment and Technology, School of Mechanical Science and Engineering, Huazhong University of Science and Technology, Wuhan 430074, China

[2] Department of Aerospace Engineering, Graduate School of Engineering, Nagoya University, Nagoya 4648603, Japan

*Corresponding author: shamoto@nagoya-u.jp, jfxu@hust.edu.cn

Abstract: In this study, a novel dynamic contour error compensation technique has been proposed for the elliptical vibration cutting process achieved through the ultra-precision amplitude control. The influence of the contour error, triggered due to the inertial vibrations of the friction-less feed drive system, on the machining accuracy deterioration has been experimentally investigated. In order to reduce the contour error, a compensation method utilizing a real-time amplitude control in the elliptical vibration cutting process has been applied. In the proposed method, the dynamic motion error along the depth of cut direction is detected by utilizing the precise linear encoders installed on the feed drive system. The motion error in real-time is subsequently converted into cancelling amplitude command for the vibration control system of the ultrasonic vibrator, thus, guaranteeing that the envelope of the vibration amplitudes auto-tracks the dynamic reference position of the motion axis in the depth of cut direction. Due to this, a constant nominal depth of cut can be obtained even though the inertial vibrations disturb the feed drive control during machining. A series of experimental investigations have been conducted in order to analyze the machining performance by employing the proposed method. The maximum machining error is observed to significantly decrease from 0.6 to 0.04 μm by applying the proposed compensation method. Finally, the micro dimple array with a structural height from about 200 to 600 nm could be accurately fabricated with a maximum machining error of 36.8 nm, which

verified the feasibility of the proposed amplitude control compensation method.
Keywords: Contour error compensation; Elliptical vibration cutting; Inertial vibrations; Micro/nano machining.

1. Introduction

With the rapid development of the advanced optoelectronics industry, the demand for the functional micro/nano structures on the optical elements is significantly increasing. For instance, the micro-lens arrays with high aspect ratio, precise alignment and significant focus uniformity are crucial for the integral imaging 3D display systems [1]. Millions of micro lenses are employed in the advanced CMOS (Complementary Metal Oxide Semiconductor) image sensor technology [2], where rays of light can be efficiently collected and focused on the optical sensors. Hence, the sensitivity of the sensor unit is efficiently enhanced. Considering the widespread use of the textured surfaces and their mass production, technologies for effective manufacturing of the functional surfaces for a variety of materials, especially steel, are required. Steel is a typical material widely used for the mechanical elements, molds and dies. The ultra-precision diamond cutting has been commonly applied to fabricate the sophisticated micro/nano structures, especially in a variety of plastic molding applications [3-6]. However, Paul et al. [7] found that the chemical affinity of the materials triggers extreme chemical reaction of the single crystal diamond (SCD) tools during machining of the ferrous materials. Due to this, the conventional diamond cutting is not applicable for the machining of steel owing to the rapid tool wear and surface deterioration. Hence, advanced diamond cutting technology is highly required for the precise machining of the steel materials. For this purpose, Shamoto and Moriwaki [8] proposed a novel cutting method named elliptical vibration cutting (EVC). The feasibility of the practical machining of the steel materials was experimentally verified by applying the ultrasonic EVC with diamond tools [9-12]. The thermo-chemical reactions between diamond and steel could be effectively suppressed, thus, resulting in successful ultraprecision machining without the development of rapid tool wear and surface quality deterioration. In another study, Suzuki et al. [13] proposed a unique micro/nano sculpturing method by precisely controlling the vibration amplitude in EVC. The depth of cut (DOC) could be changed accurately and swiftly without Fast

Tool Servo (FTS), while being controlled by the conventional FTS technology. One of the unique advantages of EVC is the inherent integration with the FTS function through amplitude control. Several micro-dimple arrays have been successfully fabricated on the hardened steel molds [13-15]. The profile accuracy of the dimples is generally in the sub-micrometer scale range. The ultra-precision machining of such a small micro dimple structure requires an extremely accurate motion control of an ultra-precision machine tool (UPMT).

The vibrations of UPMT should be mitigated to achieve the geometrical accuracy requirements in the micro/nano machining process. In general, UPMTs are mounted on the passive/active vibration isolators to cancel the effect of the ground vibrations [16, 17]. The passive isolators are cost efficient as these rely on the pneumatic dampers. Hence, these are greatly favored in the industry for practical applications. However, a major disadvantage of the passive vibration isolators is their low stiffness, which makes it difficult to support the inertial forces of each axis in motion. In other words, the machine table is supported by the soft springs provided by the pneumatic vibration isolators. In case the motion of the machine tables is accelerated or decelerated, the inertial forces of the machine table excite the vibration of the machine structure itself, thus, triggering the low frequency rocking modes [18, 19]. These vibrations subsequently cause the relative motion in the form of tracking errors between the tool and workpiece. Hence, the dynamic contour errors are generated on the workpiece, thus, deteriorating the finished surface [20]. The low frequency structural mode of each axis of motion can be approximated as an under-damped second order system [21]:

$$G(s)=\frac{{\omega_n}^2}{s^2+2\zeta\omega_n s+{\omega_n}^2} \tag{1}$$

where ω_n and ζ are the natural frequency and damping ratio. It should be noted that the UPMT drives are typically designed based on the linear motor drive systems. Due to the lack of the transmission ratio with extremely low friction, the feedback servo system cannot reject the onboard disturbance forces. As a result, these low frequency rocking vibrations of the machine, caused by the inertial reactions with the moving machine components, can easily affect the tracking accuracy of UPMTs. Hence, the suppression

of the machining error, caused by the inertial vibrations, is one of the most important challenges in the ultra-precision micro/nano machining.

In practice, the triggering of these vibrations can be avoided by generating the smooth reference motion trajectories within the control system [22]. Most UPMTs utilize the jerk limited or bell-shaped acceleration profiles to generate the smooth motion commands. Though these techniques are effective in avoiding most of the structural vibrations, however, these cannot mitigate the rocking vibrations in the range of lower than 10-20 Hz. The advanced servo systems utilize the notch filters to remove the frequency components of the reference trajectory in this region. Another technique for this purpose is to utilize a FIR (finite impulse response) filtering based trajectory generation technique [19, 22]. These techniques are observed to be effective as long as the resonance frequency is accurately identified in advance. It should be noted that due to the various workpiece inertias, the application of the notch or FIR filtering based trajectory generation may not be robust. Therefore, an active damping of these vibrations becomes crucial in attaining the high positioning accuracy. However, the active damping by solely using the existing feed drives in the machine tool suffers from the instability issues. For this purpose, Dumanli and Sencer designed a non-collocated control system to dampen the unwanted ball-screw vibrations [23]. The tracking and vibration attenuation should be balanced in an optimal control framework. Hence, it is critical to develop the techniques compensating for the unwanted vibrations, without sacrificing the stability and performance of the servo control system. As reported by Zhu et al. [24], the FTS technology can be applied for the precision positioning of the tool insert during machining. This way, the motion accuracy compensation in machine tool industry can be achieved. In another study, Gao et al. [25] compensated the motion error of a diamond turning machine through the FTS unit by employing the measurement results. Kim and Kim [26] also developed an FTS unit to compensate the thermal growth error of a spindle with a saw-tooth shape. The contour error was observed to be efficiently reduced by the compensatory FTS motion in real time, which followed the negative output of a capacitive displacement sensor for measuring the flatness of the machined surface. As mentioned above, the micro-dimple array is fabricated by the amplitude control sculpting method in

EVC [13], and the depth of the cut can be changed rapidly while being controlled by the conventional FTS technology. The EVC technology is equipped with an FTS function by itself. It is assumed that the amplitude control sculpturing method is one of the potential solutions to compensate the dynamic contour error mainly caused by the inertial vibrations of the machine tools.

In the above-mentioned literature studies on accuracy compensation with FTS [25, 26], the external sensors and target artifact have been used to effectively calibrate the relative displacement of the machined workpiece. However, the external sensors are considerably sensitive to the changes in the environmental conditions such as temperature, humidity and electromagnetic interference. It is challenging to reduce the measurement noise during the machining processes, which causes the capability deterioration in the contour error feedback or compensation. Moreover, the external sensor also enhances the cost and complexity of the manufacturing systems. Recently, the ultra-precision machine tools have been equipped with a number of internal sensors. For instance, a variety of high-precision and high-resolution encoders and linear grating scales have been adopted to monitor the position of each axis in real time [27]. In our machine tool reported here, the dynamic position error, mainly caused by the inertial vibrations, can be quantified by the linear encoder. To overcome the dynamic contour error generated due to the machine inertial vibration, the ultra-precision amplitude control sculpturing method has been adopted to EVC. The position error is subsequently changed into an input command in real time for controlling the vibration amplitudes. Hence, it leads to the effective cancellation of the inertial vibrations of the machine tool by applying the amplitude control sculpturing method in EVC. In order to verify the proposed dynamic contour error compensation method for improving the machined profile accuracy, the experimental investigations have been conducted in the present study. Firstly, the elliptical vibration cutting process has been roughly explained. Secondly, the inertial vibrations in the motion axis of the ultra-precision machine tool have been investigated through the fundamental planing motion without cutting. Thirdly, the influence of the inertial vibrations on the machined profile accuracy has been evaluated through the flat surface machining and micro-dimple array machining process. Based on

the experimental investigations, the amplitude control compensation method in EVC has been subsequrntly introduced. Finally, the flat surface machining and micro-dimple array fabrication on the hardened steel has been conducted with the proposed compensation method in order to verify the feasibility of the proposed dynamic contour error compensation. The ultra-precision machining with high machining efficiency and accuracy have been demonstrated through the proposed method.

2. Amplitude control sculpturing method in EVC

Figure 1 schematically illustrates the EVC process [8]. In the EVC process, the cutting tool vibrates elliptically and feeds along the nominal cutting direction. To ensure the complete separation of the tool from the workpiece during each vibration cycle, the nominal cutting speed is usually lower than the maximum vibration speed in the nominal cutting direction. Due to the separation of the tool workpiece during each vibration cycle, the newly developed and chemically active back surface of the chip is exposed to the surrounding gas and/or cutting fluid, which reduces the chemical activity and suppresses the thermo-chemical adhesion/diffusion wear of the cutting tools. Some ultrasonic elliptical vibration tools have been developed so far, and their optimal performance in steel machining has been industrially verified by applying the SCD tools [9, 10].

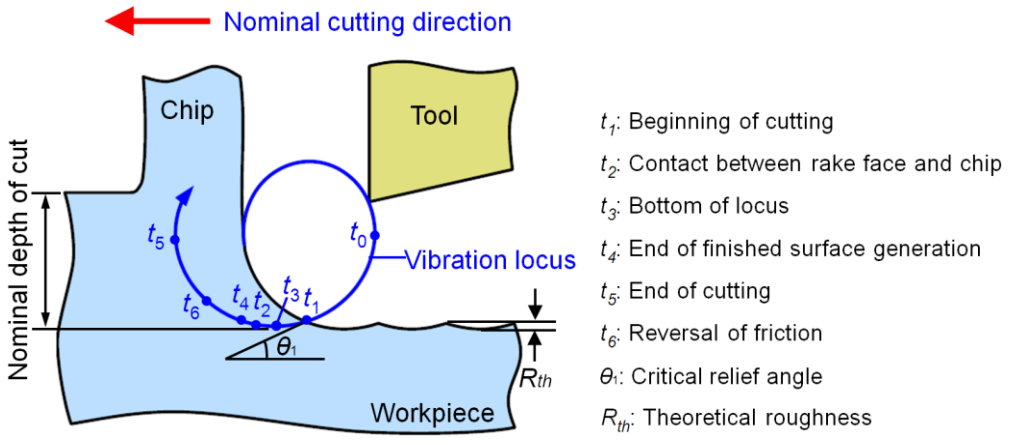

Fig. 1. Elliptical vibration cutting (EVC) process [8].

Based on the successful cutting performance associated with EVC in the practical applications, the unique micro/nano sculpturing method by amplitude control has been

proposed, as shown in Fig. 2 (a).

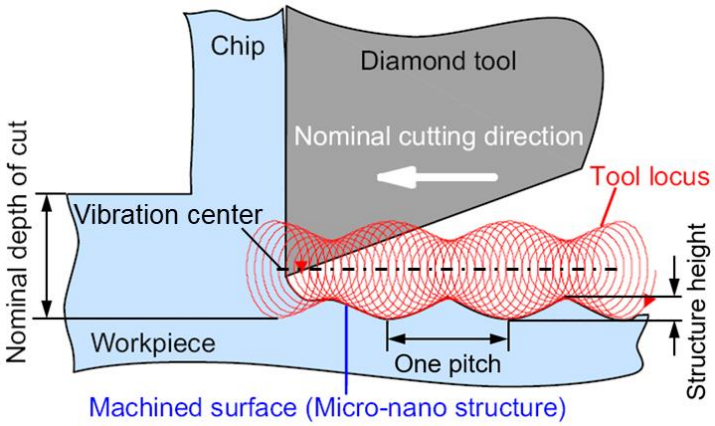

(a) Amplitude control sculpturing method in the EVC process [13].

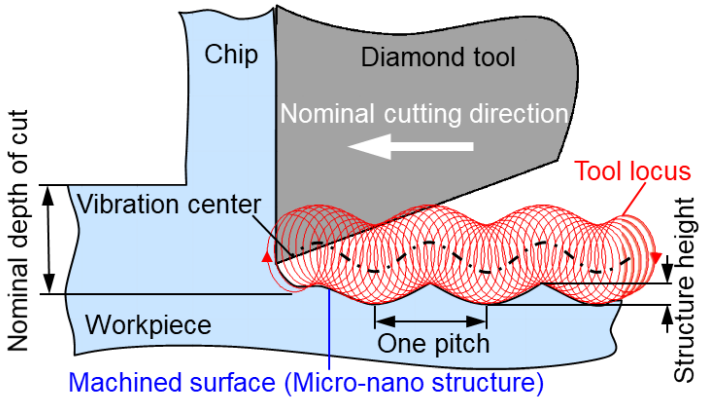

(b) Sculpturing method combining EVC with the conventional FTS.

Fig. 2. (a) Proposed amplitude control sculpturing method in EVC [13] and (b) sculpturing method combining EVC with the conventional FTS.

The vibration amplitude can be accurately and swiftly controlled during machining. The amplitude variation in the depth of cut direction triggers almost identical variation in the depth of cut. Hence, the depth of cut can be changed while being controlled by the conventional FTS technology. Through primary experimental studies, the feasibility of the amplitude control sculpturing method in EVC was effectively verified in the micro/nano machining of the steel materials with SCD tools [13-15]. In the proposed amplitude control sculpturing method, the trajectory of the vibration center maintains a straight line, as shown in Fig. 2 (a). Similar sculpturing performance may be attained by

utilizing the conventional FTS technology, where the trajectory of the vibration center fluctuates without changing the vibration amplitudes, as shown in Fig. 2 (b). It is, however, not advantageous to combine the elliptical vibration tool with the conventional FTS, as both devices already contain a function for swiftly changing the depth of cut [13,14]. In other words, the EVC technology already comprises of an inherent FTS function.

As introduced in our previous research study [14], the proposed amplitude control sculpturing method imposes several restrictions on the machinable part geometry due to the specific nature of the EVC process. For instance, the structural height can be controlled within the maximum value of the mean-to-peak amplitude in the depth of cut direction. Additionally, the curvature radius of the target profile should be larger than that of the vibration locus. Moreover, the amplitude command and resultant envelope do not fully correspond to each other, especially at the regions with steep slopes due to the presence of the finite amplitude in the nominal cutting direction, as shown in Fig. 3 (a). Hence, a command compensation method is usually applied to achieve the target structure machining, as illustrated in Fig. 3 (b). In each vibration cycle, the vibration locus is tangential to the target profile so as to suppress the machining error. With the elliptical vibrator, the vibration amplitude can be controlled within the frequency bandwidth of about 300 Hz. This frequency bandwidth is relatively narrow as compared to the conventional FTS. However, it might not be a significant challenge due to the relatively low nominal cutting speed in the EVC technology.

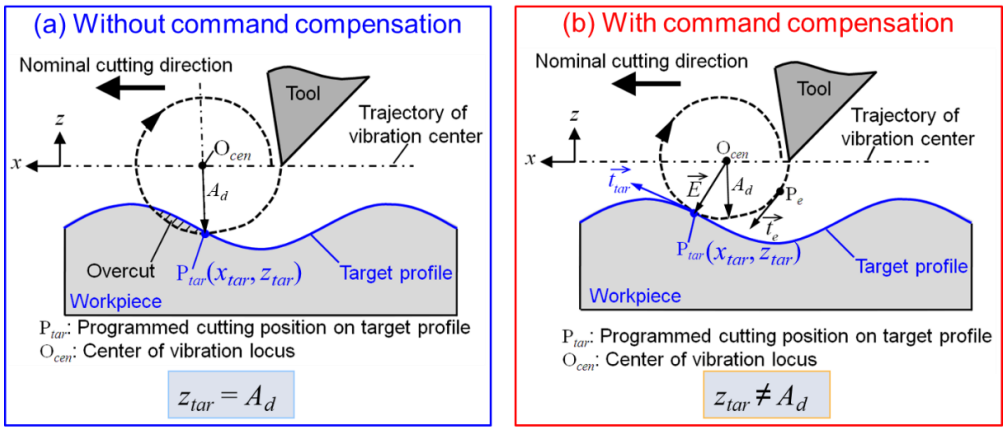

Fig. 3. Amplitude control sculpturing method (a) without and (b) with command compensation (A_d: Vibration amplitude in DOC direction; $P_{tar}(x_{tar}, z_{tar})$: Target position)

3. Influence of inertial vibrations of motion axis on machining accuracy

3.1 Inertial vibrations of motion axis in depth of cut direction

In order to quantitatively analyze the dynamic inertial vibrations in the motion axis, a fundamental planing motion consisting of the simple stop and go straight motions was experimentally investigated. The ultra-precision machine tool, ASP01UPX, developed by Nachi-Fujikoshi Corp., was used for this purpose. It had a position command resolution of 1 nm and motion straightness of <0.1 μm over 100 mm in each linear axis. Considering the arrangement of the adopted ultra-precision machine tool, each stroke in the planing process was introduced in detail, as shown in Fig. 4.

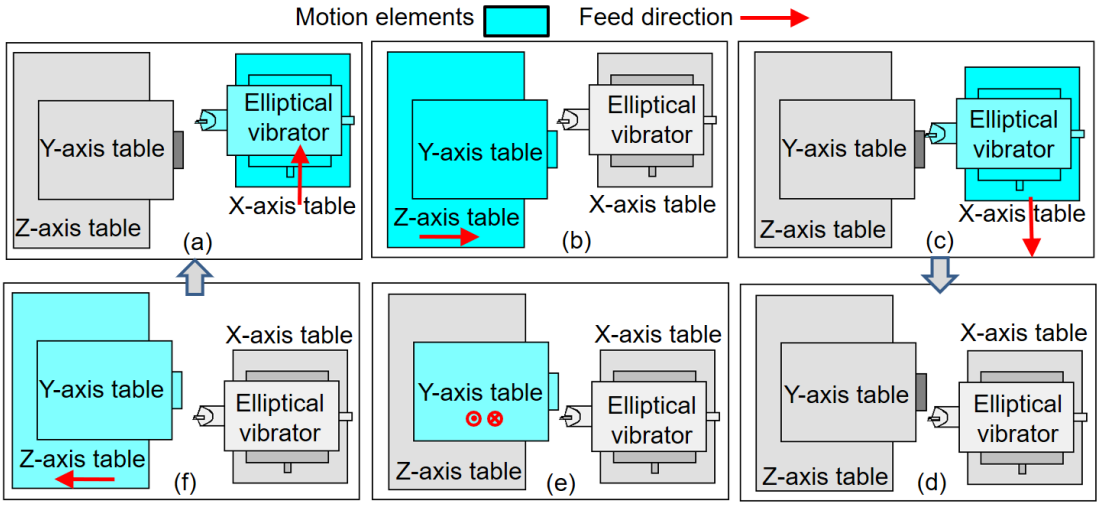

Fig. 4. Schematic of the planing process (a) Tool retraction (b) DOC control (c) Planing stroke (d) End of planing stroke (e) Pick feed control (f) Relieving of the tool.

In the ultra-precision machine tool, a set of the linear motor and hydrostatic guideway advantageous for the high motion accuracy and high feed rate is utilized. Due to the stacked machine tool structure with the Y-axis table mounted on the Z-axis table, the total mass of the Z-axis becomes non-negligible with respect to the machine tool itself. Therefore, the acceleration/deceleration motion of the Z-axis correspondingly excites the rocking mode vibration of the machine tool. As the linear motor drive system of the ultra-precision machine tool has a small transmission ratio and low friction of hydrostatic guideways, the rocking mode vibration subsequently triggers the inertial vibrations of the Z-axis table with low damping. As the cutting tool penetrates into the

workpiece at Fig. 4 (c), thus, the machining accuracy is determined by the motion accuracy in the planing step. The cutting depth is directly affected by the residual vibration in the previous neighbor motion process, i.e., positioning motion of the Z-axis for depth of cut control, as shown in Fig. 4 (b). Hence, the effect of the inertial vibration of the Z-axis table on the machining accuracy should be explored in detail. In the present study, the stroke distance of the Z-axis in Fig. 4 (b) has been set to a small value of 0.3 mm, with the feed speed command of the Z-axis chosen to be a relatively high value of 1 m/min to achieve a shorter process time, i.e., highly efficient machining.

Firstly, the dynamic motion error caused by the inertial vibration of the Z-axis table was experimentally evaluated. The planing motion was adopted without machining, as shown in Fig. 4. Figure 5 (a) shows the setup for measurement of the inertial vibration of the Z-axis table along the DOC direction.

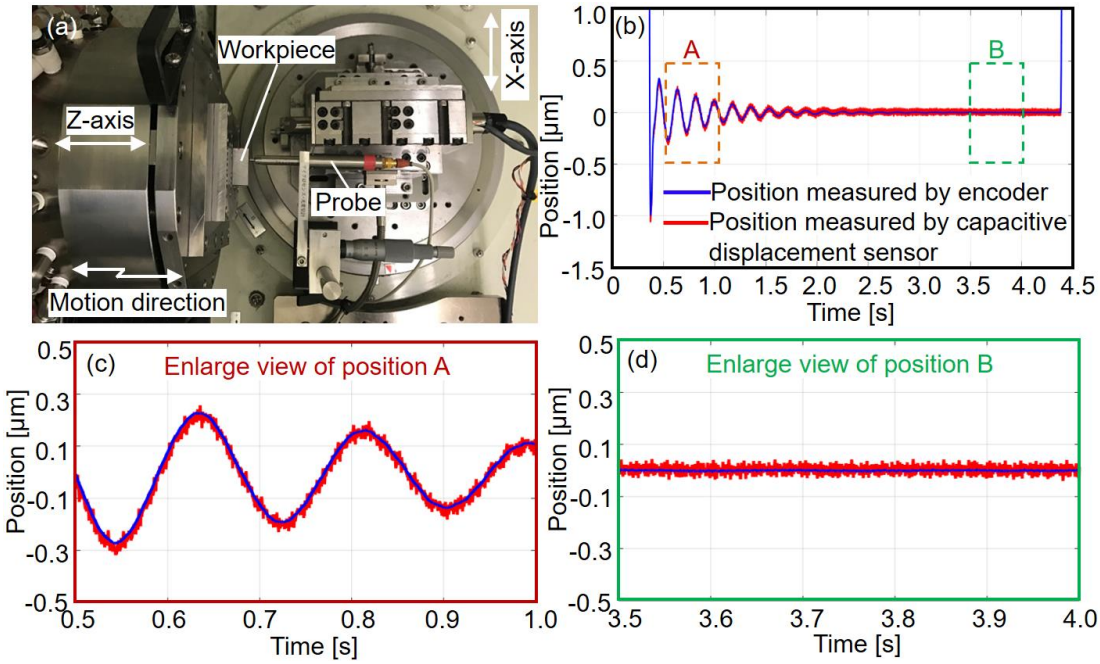

Fig. 5. Experimental setup and measurement results of inertial vibrations in Z-axis.

Relative displacement of the Z-axis table against the tool post on the X-axis table is measured by a capacitive displacement sensor (MicroSense 5430). The measurement resolution of this sensor is observed to be about 3 nm, with measurable working distance of ±15 μm and dynamic bandwidth of about 1 kHz. The sensor is fixed on the X-axis

table. During the demonstrative motion, a reciprocating feed motion is provided on the Z-axis table for achieving the depth of cut control. To explore the measurement capability of the position encoder inside the machine tool, the dynamic motion position of the Z-axis table is also detected by the encoder in real time. Figure 5 (b) shows the inertial vibrations of the Z-axis table measured through the capacitive displacement sensor and encoder, respectively. The positions measured with these entities are observed to agree well with each other, as shown the enlarged views in Figs. 5 (c) and (d). The position encoder inbuilt in the machine tool can precisely detect in real time the dynamic motion error triggered by the inertial vibrations of the Z-axis table. Moreover, the measurement noise from the encoder is negligible and can be adopted as a control command directly to achieve FTS control without filtering. Figures 5 (b) and (c) also indicated that the maximum peak-to-valley amplitude of the inertial vibrations is ~0.6 μm with a dominant rocking frequency of ~5 Hz. As the mean-to-peak amplitude of the developed elliptical vibrator can be arbitrarily controlled within 0-2 μm with a bandwidth of about 300 Hz [13], it becomes feasible to apply this elliptical vibrator to the contour error compensation.

3.2 Inertial vibrations in DOC direction on contour error generation

The experimental investigations were subsequently carried out in order to verify the influence of inertial vibrations on the dynamic contour error. The planing motion, as shown in Fig. 4, was adopted with real machining. Figure 6 shows the experimental setup.

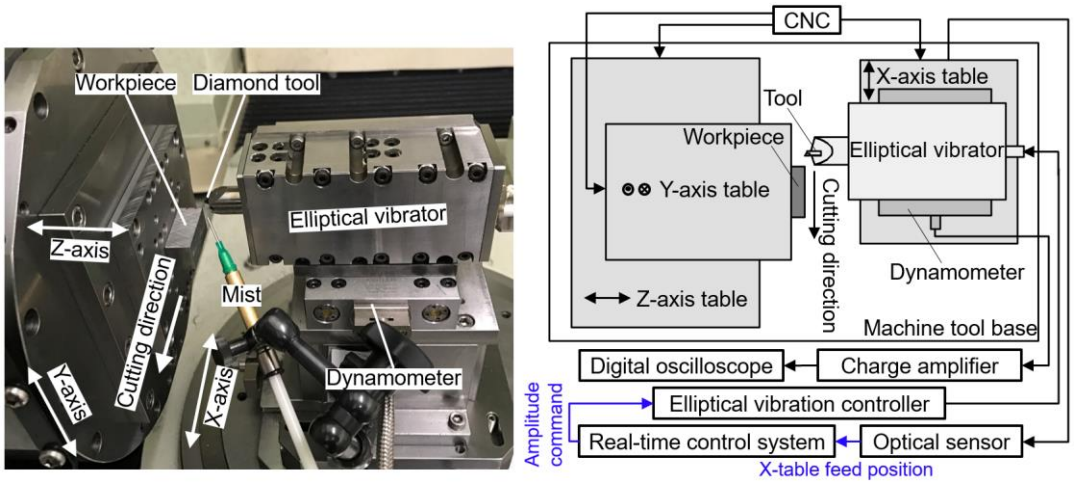

Fig. 6. Illustration of the experimental setup.

A two-degree-of-freedom (2-DOF) elliptical vibrator developed in collaboration with Taga Electric Co., Ltd. is attached to the X-axis table. The vibration amplitude in the depth of cut direction along the Z-axis is controlled in synchronization with the feed motion of the X-axis. The vibrator can generate the longitudinal and bending vibrations simultaneously at the ultrasonic frequency of ~36.2 kHz. Thus, a 2-DOF elliptical vibration can be obtained at the diamond tool tip attached to the vibrator. The mean-to-peak amplitude of 0-2 μm can be arbitrarily controlled in the DOC direction with a bandwidth of ~300 Hz by using the external command voltage [13]. A SCD tool with a nose radius of 1 mm, rake angle of 0º and clearance angle of 10º is used. Table 1 shows the experimental conditions, including the details for the flat surface machining and micro dimple fabrication.

Table 1 Experimental conditions for flat surface machining and micro dimple fabrication

Conditions		A (Flat surface)	B (Micro dimple)
Elliptical vibration conditions	Frequency [kHz]	36.2	
	Amplitude in cutting direction [$\mu m_{0\text{-}p}$]	2	
	Amplitude in DOC direction [$\mu m_{0\text{-}p}$]	2	1-2
	Phase shift [deg]	90	
Cutting conditions	Depth of cut [μm]	5	0.3
	Cutting speed [mm/min]	180	
	Pick feed [μm]	20	130
Tool	Material	SCD	
	Nose radius [mm]	1	
	Rake angle [deg]	0	
	Clearance angle [deg]	10	
Workpiece	Material	JIS: SUS420J2 (HRC 53)	

A short air-cut distance of about 0.15 mm is adopted in the nominal cutting direction during the experimental investigation, and no dwell time exists for the motion axis in each planing stroke. Therefore, the cutting starts immediately after the Z-axis motion. Such a continuous operation is preferable with respect to the reduction of the travel time. However, the inertial vibration is occasionally challenging to be dampened before the tool approaches the workpiece. It is assumed that the inertial vibrations of the Z-axis

table can be transferred on the machined surface relatively easily. Figure 7 shows the microphotograph and measured profile of the flat surface machined under conditions described in subset A. Due to the inertial vibrations, the machined profile assumes a damped vibration shape. The peak-to-valley value of the profile is measured to be about 0.65 μm, which is close to the measured peak-to-valley amplitude of the inertial vibrations of the Z-axis table shown in Fig. 5.

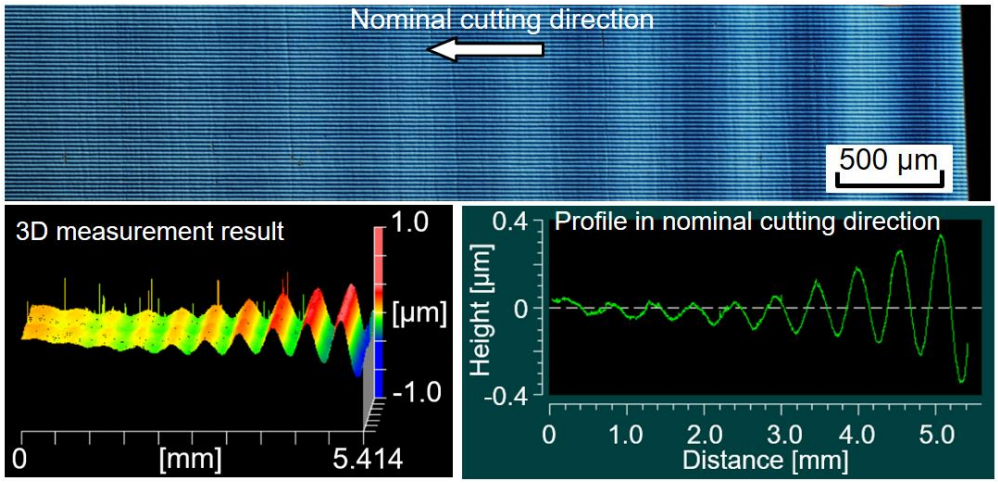

Fig. 7. The flat surface machined with inertial vibrations in the DOC direction.

Next, the influence of the inertial vibration in the micro dimple machining process is investigated. Fig. 8 demonstrates the detailed amplitude control sculpturing method for the fabrication of micro dimple on the hardened steel (SUS420J2, HRC53) [13].

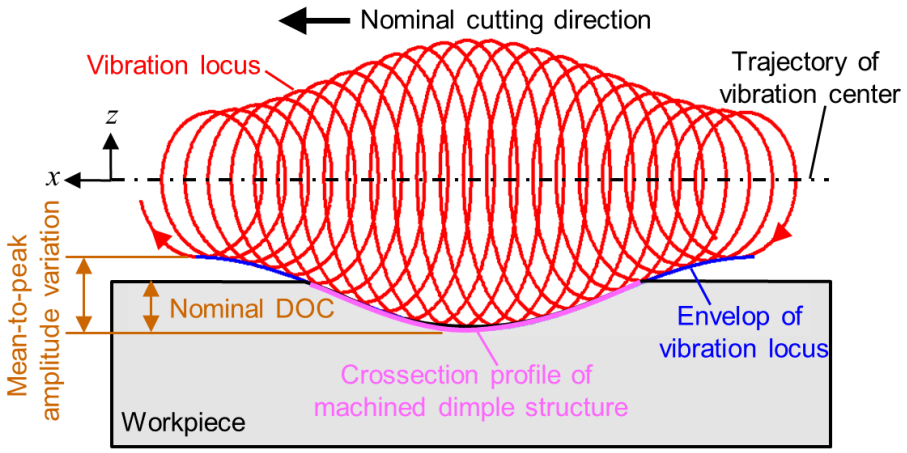

Fig. 8. Amplitude control sculpturing method for micro dimple fabrication.

The vibration amplitude is controlled in synchronization with a simple planing motion of the ultra-precision machine tool. The independent micro dimple can sunsequently be fabricated with a small nominal DOC value, which is less than the mean-to-peak amplitude variation in the DOC direction. Finally, the bottom phase of the vibration locus envelop is transferred as the micro dimple. Figure 9 shows the microphotograph and measured profile of the dimple array fabricated by the conditions mentioned in subset B.

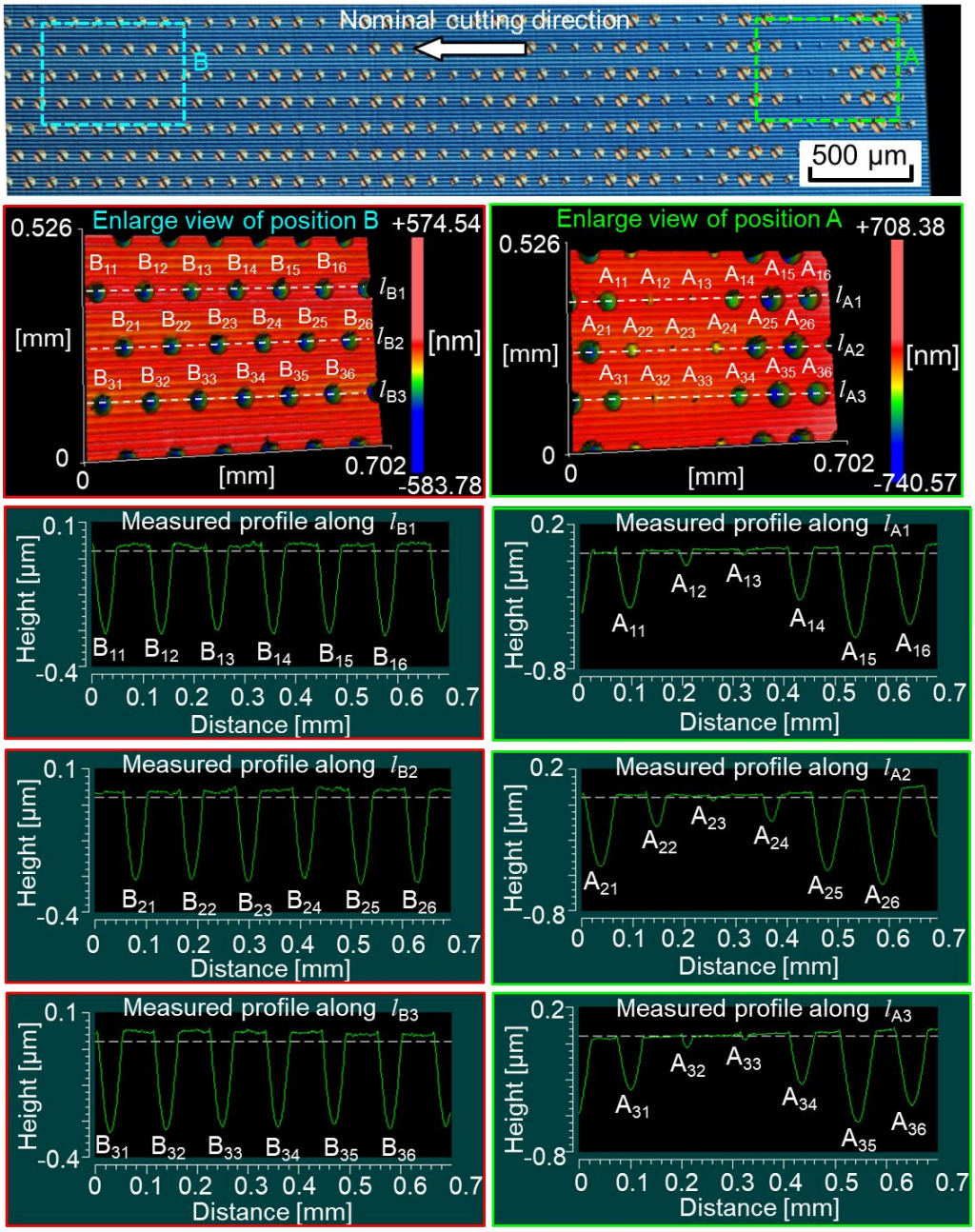

Fig. 9. Micro dimple fabricated with the inertial vibrations in the DOC direction.

A small nominal DOC value of 0.3 μm, less than half of the mean-to-peak amplitude variation of 1 μm, is adopted. Due to the inertial vibrations of the Z-axis table, the geometrical properties of the fabricated micro dimples significantly deteriorate at the beginning of the cutting process (Position A), as shown in Fig. 9. The cross section profile of the fabricated dimples in three neighbour cutting strokes was investigated at Position A. Each dimple is numbered as A_{ij}, where i=1, 2 and 3, j=1, 2, 3, 4, 5 and 6. The structural depth of these fabricated dimples is summaried in Table 2. At the beginning of each cutting stroke, the average structure depth is measured to be about 0.3569 μm (average value of 0.3499 μm, 0.3893 μm and 0.3306 μm in Table 2) at the Position A in Fig. 9. The average standard deviation σ_A of the structural depth is about 0.2167 μm (average value of 0.2140 μm, 0.2207 μm and 0.2155 μm in Table 2). As comapred with the designed structural depth of 0.3 μm, an average machining error of 0.0569 μm is generated in the structural depth. Moreover, a maximum machining error of 0.3756 μm is generated with considering the measured prolife along l_{A2}.

Table 2 Structural depth at the beginning of cut without compensation [μm]

A	j=1	j=2	j=3	j=4	j=5	j=6	Average value	Standard deviation σ_A
i=1	0.4046	0.1134	0.0402	0.3602	0.6340	0.5473	0.3499	0.2140
i=2	0.5480	0.2571	0.0623	0.2225	0.5702	0.6756	0.3893	0.2207
i=3	0.3716	0.0768	0.0345	0.3552	0.6322	0.5131	0.3306	0.2155

On increasing the machining time or cutting distance in a single planing stroke, the inertial vibrations of the Z-axis table become weak. At Position B in Fig. 9, the influence of the inertial vibrations on the nominal DOC variation is observed to be negligible. Table 3 summaries the structural depth of these fabricated dimples at Position B. The average structural depth is measured to be about 0.3052 μm (average value of 0.3076 μm, 0.3040 μm and 0.3038 μm in Table 3), where an average machining error of 0.0052 μm is generated in the structural depth. The average standard deviation σ_B of the structural depth is about 0.0042 μm (average value of 0.0043 μm, 0.0046 μm and 0.0036 μm in Table 3). A maximum machining error of 0.0136 μm is generated with considering the

measured prolife along l_{B1}. As comparing the Position A in Fig. 9 with the affection of inertial vibrations, the average machining error is decreased from 0.0569 μm into 0.0052 μm, the maximum machining error is decreased from 0.3756 μm into 0.0136 μm and the average standard deviation is decreased from 0.2167 μm into 0.0042 μm at Position B without the inertial vibrations of Z-axis. Thus, the micro- dimple array with uniform geometrical parameters can be successfully fabricated by applying the amplitude control sculpturing method. Hence, it is crucial to reduce the influence of the inertial vibrations on the profile accuracy deterioration in the highly-efficient micro/nano manufacturing process.

Table 3 Structural depth at stable cutting process without compensation [μm]

B	j=1	j=2	j=3	j=4	j=5	j=6	Average value	Standard deviation σ_B
i=1	0.3136	0.3000	0.3107	0.3071	0.3090	0.3053	0.3076	0.0043
i=2	0.3090	0.3026	0.3024	0.2964	0.3103	0.3036	0.3040	0.0046
i=3	0.3026	0.3084	0.2974	0.3076	0.3039	0.3032	0.3038	0.0036

4. Proposed dynamic contour error compensation

Figure 10 shows the machining error description in the cutting process.

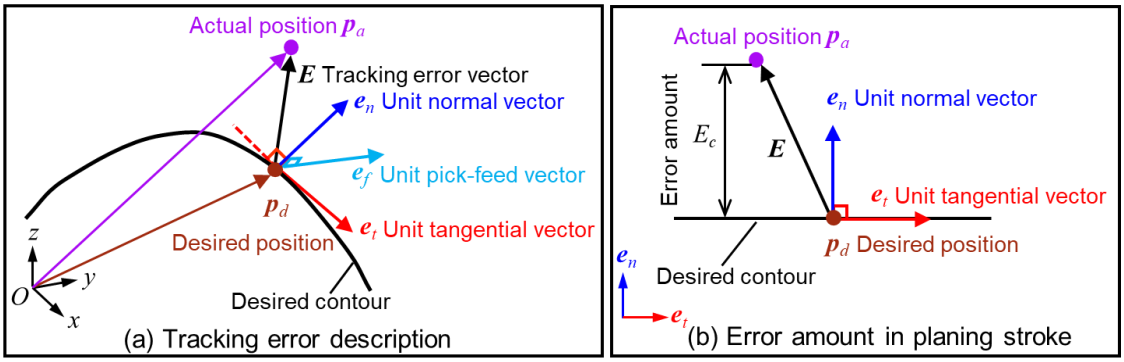

Fig. 10. Machining error description.

In Fig. 10 (a), $\boldsymbol{p}_d=[x,y,z]^T$ represents a position vector on the desired contour path at time t. A unit tangential vector of the contour path at position $\boldsymbol{p}_d$ is given as $\boldsymbol{e}_t=\frac{\partial \boldsymbol{p}_d}{\partial t}/\left|\frac{\partial \boldsymbol{p}_d}{\partial t}\right|$. At the same time, a unit vector along the pick feed direction is denoted as

$\boldsymbol{e}_f$. The unit normal vector to the machining surface can be derived as $\boldsymbol{e}_n=\boldsymbol{e}_t\times\boldsymbol{e}_f$. Hence, the error compensation amount, i.e., depth of cut error, is calculated as $E_c=(\boldsymbol{p}_a-\boldsymbol{p}_d)\cdot\boldsymbol{e}_n$. In the current study, a fundamental planing motion was adopted, as shown in Figs. 4 and 6. The desired contour path is a straight line parallel to the unit tangential vector $\boldsymbol{e}_t$ along the nominal cutting direction, as shown in Fig.10 (b). Thus, the depth of cut direction becomes identical to the normal direction on the machining surface $\boldsymbol{e}_n$. Therefore, the contour error E_c can be considered as the motion error of the Z-axis along the depth of cut direction. With the proposed experimental set up, the controllable direction of the vibration amplitude $\boldsymbol{e}_a$ is observed to be identical to the normal direction on the machining surface $\boldsymbol{e}_n$, and the amplitude compensation amount becomes equal to E_c. Otherwise, the amplitude compensation amount should be modified by using $C=E_c/(\boldsymbol{e}_a\cdot\boldsymbol{e}_n)$. On decreasing the contour error by changing the vibration amplitude in the depth of cut direction, a high machining accuracy can be guaranteed. As described in Section 3.1, the encoder detects the accurate position on each drive axis. By utilizing the servo information, not only the actual motion position but also the command position can be obtained. Due to this, the dynamic position error of each motion axis can be detected in real time. Figure 11 shows the position, reference command position and position error of the Z-axis table measured in the planing motion.

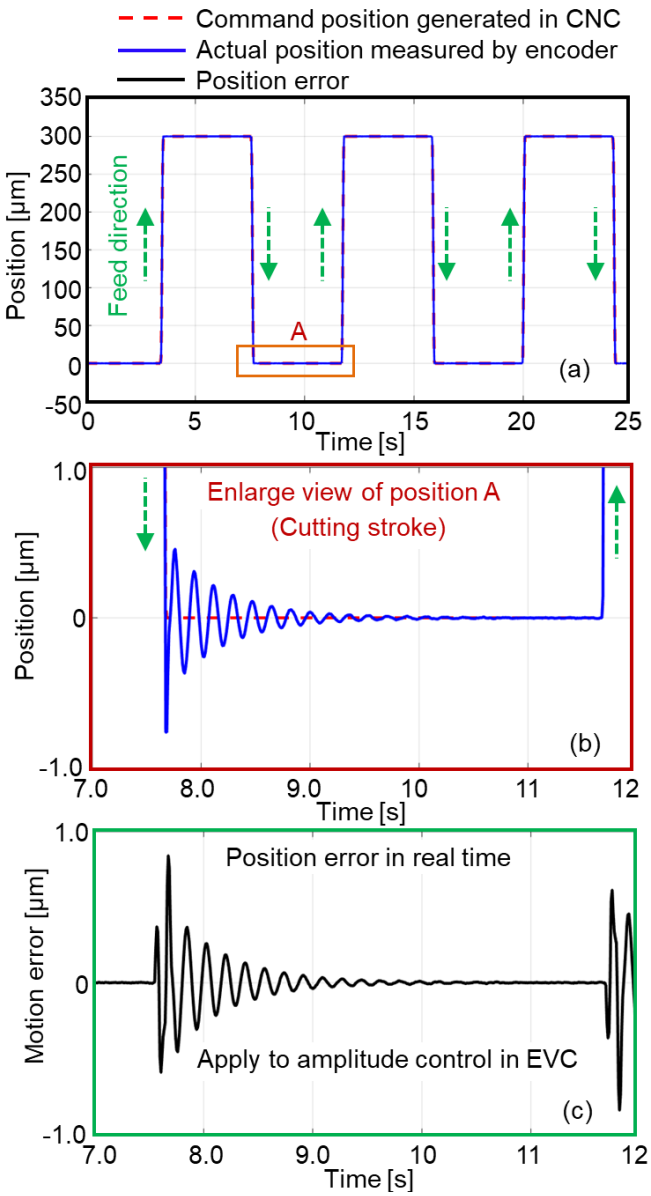

Fig. 11. The (a) actual motion position, (b) referenced command position and (c) position error of the Z-axis table in planing.

In each cutting stroke, the position error, as shown in Fig. 11 (c), can be detected in real time by using a highly precise linear position encoder with a position resolution of ~0.034 nm. The position error is subsequently converted into a voltage command and is input into a high-speed real-time control system (dSPACE) for achieving the vibration amplitude control in synchronization with the X- and Z-axes feed motion. Hence, compensating the dynamic motion error of the Z-axis table allows the control of the vibration amplitude in real time. The variation of the vibration amplitude auto-tracks the

dynamic motion position of the Z-axis table for maintaining a constant designed nominal DOC values. Figure 12 shows the conceptual schematic of the proposed contour error compensation method by applying the amplitude control in the EVC process.

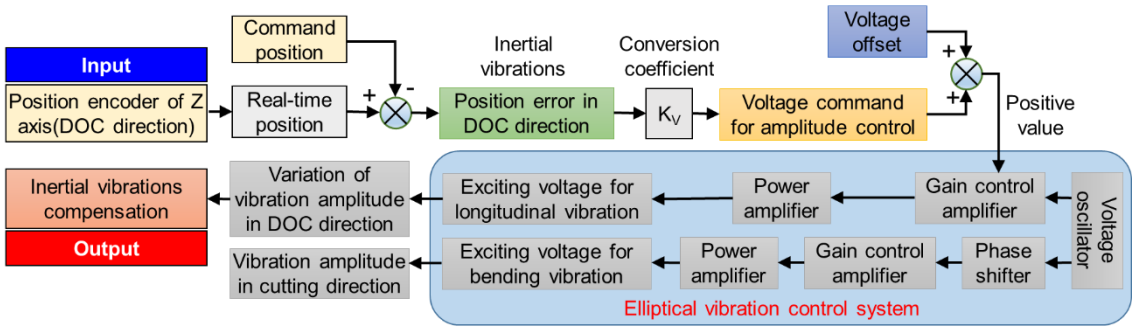

Fig. 12. Conceptual schematic of the proposed contour error compensation method.

By employing the proposed contour error compensation method, Figure 13 demonstrates the cutting edge trajectory considering the inertial vibrations of the Z-axis table in each cutting stroke.

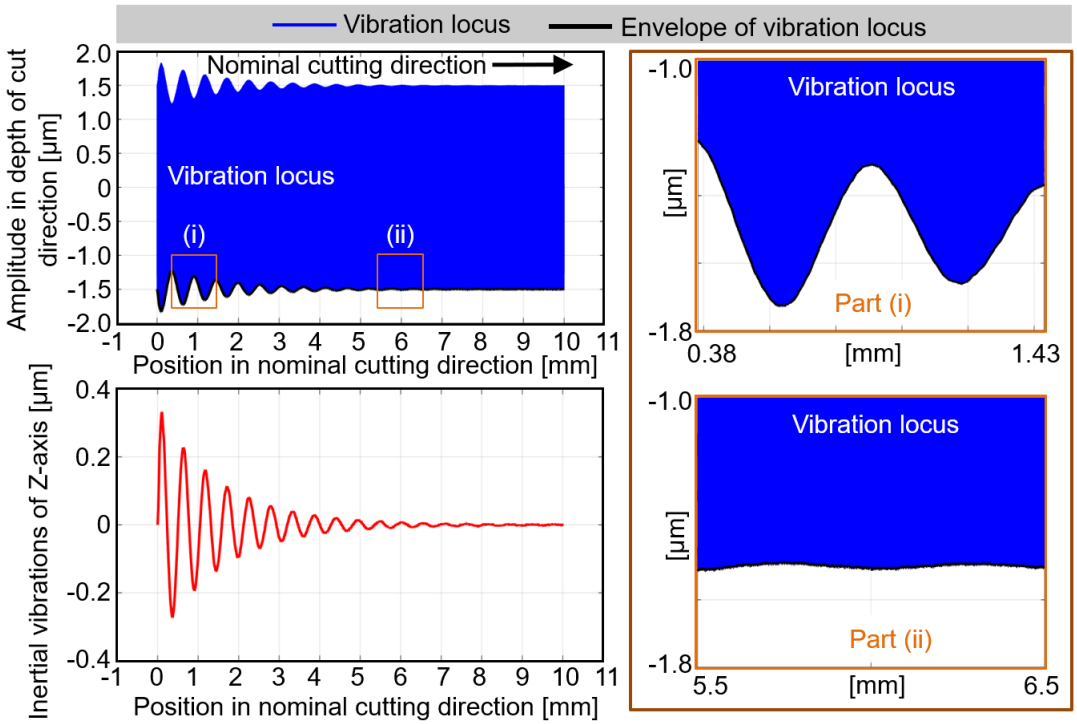

Fig. 13. Cutting edge trajectory in the proposed compensation method.

The envelope of the vibration locus follows the negative zone of the inertial

vibrations, which lets the tool tip trace the workpiece surface for maintaining the constant nominal DOC. It should be noted that the elliptical vibration frequency is 36.2 kHz, and the mean-to-peak amplitude in DOC direction varies ~1.5 μm, while the mean-to-peak amplitude in the nominal cutting direction is fixed to 2 μm. Moreover, a nominal cutting speed of 180 mm/min is adopted.

5. Experimental verification of the proposed error compensation method

The proposed error compensation method was first applied for the machining of a flat surface, as illustrated in Fig. 4. For each cutting stroke, the cutting edge trajectory is controlled, as shown in Fig. 13. Subsequently, the morphology and profile of the machined surface at the beginning of each planing stroke were investigated. Figure 14 shows the machining results with and without the contour error compensation, along with the measured profiles. The contour error is observed to decrease significantly from ~0.65 μm_{p-v} to 0.04 μm_{p-v} with the proposed compensation method. Through experimental verification, the proposed compensation method was conformed to be effective for preventing the contour accuracy deterioration due to inertial vibrations of the Z-axis table.

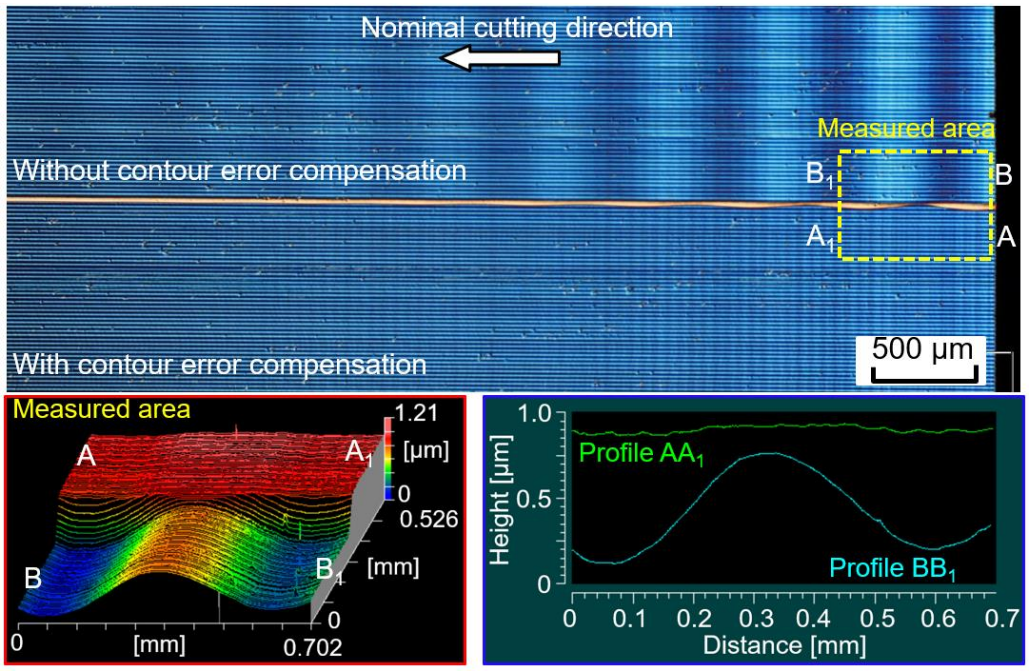

Fig. 14. Comparison of the flat surface machining without and with the proposed contour error compensation method.

The proposed contour error compensation method has been subsequently applied for the micro- dimple array fabrication. In each cutting stroke, the original command wave, i.e., sinusoidal wave as shown in Fig. 15 (a), for the vibration amplitude control in the DOC direction is modified considering the contour error caused by the inertial vibrations of the Z-axis table. Figure 15 (c) shows the compensated command wave for the amplitude control during the micro dimple fabrication. It represents the superposition of the original command wave in Fig. 15 (a) and measured contour error wave in real time shown in Fig. 15 (b). The final vibration and envelope of vibration loci for the micro dimple fabrication can be obtained, as shown in Fig. 15 (d). In each cutting stroke, the maximum nominal DOC almost retains a constant value, although the inertial vibrations of the Z-axis table in the DOC direction are generated.

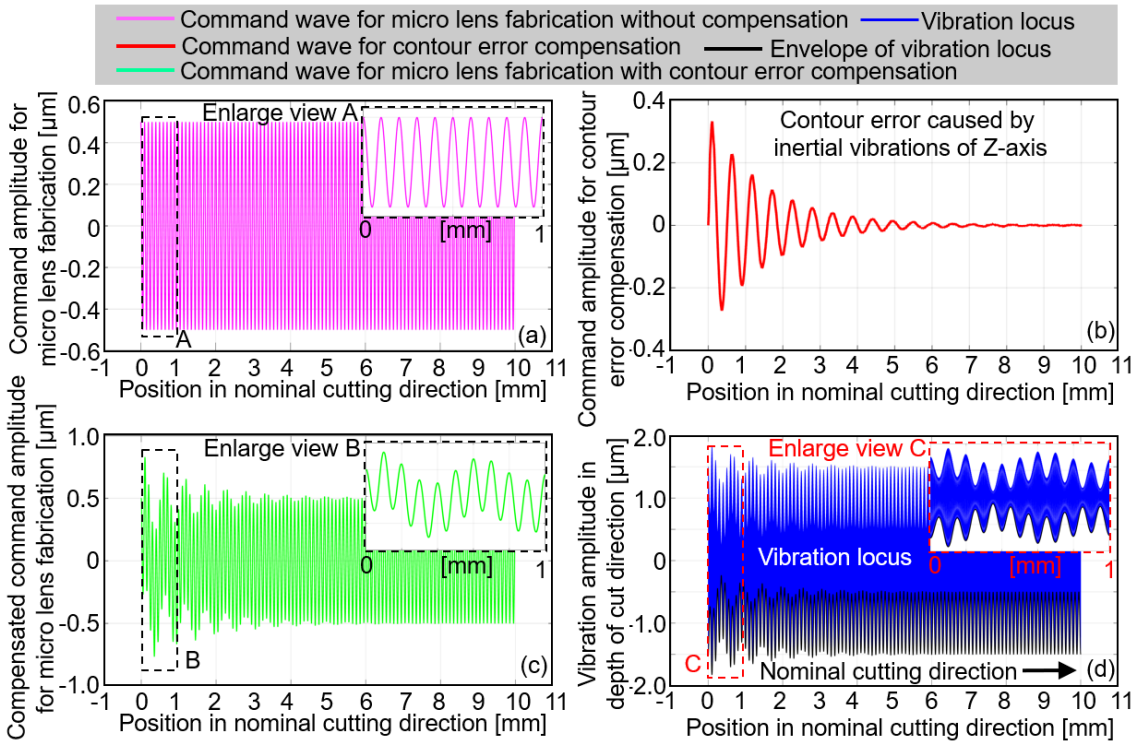

Fig. 15. Application of the contour error compensation method in micro dimple fabrication.

Figure 16 shows the microphotograph and measured profile of the micro-dimple array fabricated using a similar condition mentioned in subset B in Table 1.

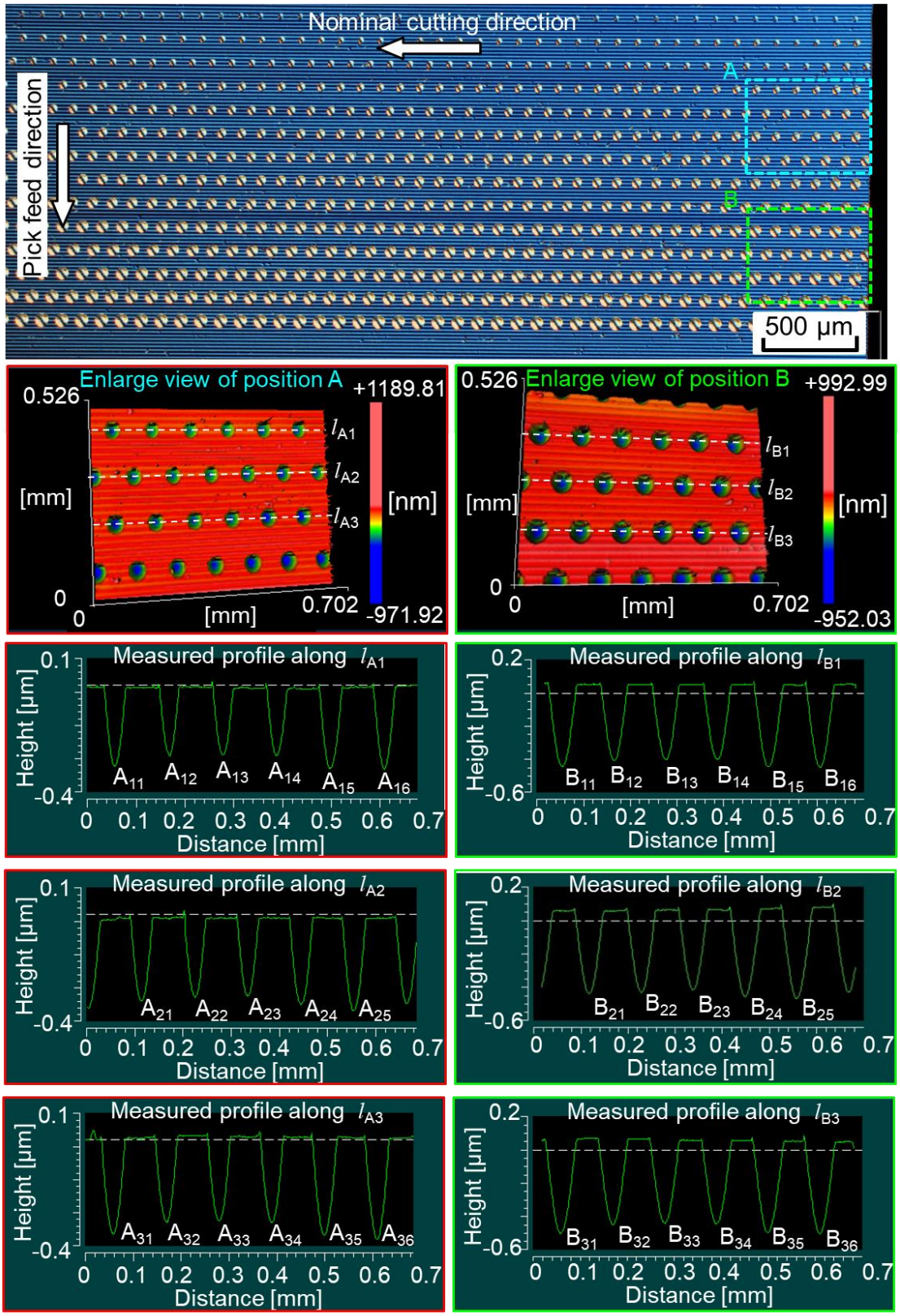

Fig. 16. Micro dimple fabrication with the proposed contour error compensation method.

The nominal DOC value is set to be gradually increased from 0.2 to 0.6 μm. Hence, the feasibility of proposed compensation methed can be experimentally verified by fabricating a series of dimples with different dimentions. The structural depth of these fabricated dimples was summaried in Table 4.

Table 4 Structural depth at the beginning of cutting stroke with compensation [μm]

	No.	j=1	j=2	j=3	j=4	j=5	j=6	Average value	Designed value	Standard deviation σ
A	i=1	0.2918	0.2544	0.2495	0.2514	0.3014	0.3023	0.2751	0.2660	0.0236
	i=2	0.3107	0.2972	0.2904	0.3239	0.3470	--	0.3138	0.2990	0.0202
	i=3	0.3651	0.3194	0.3137	0.3196	0.3688	0.3851	0.3453	0.3320	0.0285
B	i=1	0.4969	0.4616	0.4507	0.4523	0.4974	0.4983	0.4762	0.4640	0.0216
	i=2	0.4974	0.4824	0.4648	0.5077	0.5225	--	0.4950	0.4970	0.0200
	i=3	0.5554	0.5022	0.488	0.4984	0.5497	0.5600	0.5256	0.5300	0.0298

At the Position A in Fig.16, the structural depth is designed to be 0.266 μm, 0.299 μm and 0.332 μm when the cross section profile of the dimples is measured along l_{A1}, l_{A2} and l_{A3} respectively. Meanwhile, the structural depth is designed to be 0.464 μm, 0.497 μm and 0.530 μm when the cross section profile is measured along l_{B1}, l_{B2} and l_{B3} respectively at the Position B in Fig.16. Based on the measurement results in Table 4, the average machining error is about 0.0093 μm in the structural depth. Furthermore, a maximum machining error of 0.0368 μm is generated with considering the measured prolife along l_{A3}. The average standard deviation σ of the structural depth is about 0.0240 μm (average value of 0.0236 μm, 0.0202 μm, 0.0285 μm, 0.0216 μm, 0.0200 μm and 0.0298 μm in Table 4). As comparing to the fabricated dimples in Fig. 9 (Position A) with the inertial vibrations affection, the average machining error is decreased from 0.0569 μm into 0.0093 μm, the maximum machining error is decreased from 0.3756 μm into 0.0368 μm and the average standard deviation is decreased from 0.2167 μm into 0.0240 μm. It means that all of these dimples can be fabricated with a maximum contour error of <0.04 μm even at the beginning of each cutting stroke. In our present research, the contour error is formally defined as the shortest distance between the reference designed

profile and actual measured profile. It means that the contour error is the deviation from the designed profile to the measured profile in the gradient direction [28]. Compared with the machining results without contour compensation, i.e., at position A in Fig. 9, the influence of the inertial vibrations on the nominal DOC variation can be efficiently reduced. Thus, the micro-dimple array with uniform geometrical parameters can be accurately fabricated by applying the amplitude control sculpturing method equipped with the proposed contour error compensation method.

6. Conclusion

The present study proposes a contour error compensation process by means of the amplitude control sculpturing method in EVC for fabricating the micro/nano structures on the hardened steel. The contour error generation, mainly caused by the inertial vibrations of the motion axis in the DOC direction, has been experimentally investigated. The error value is observed to be close to the feature size of the designed micro/nano structures in the DOC direction, which exerts a significant influence on the geometrical deterioration of the fabricated structures. In order to reduce the contour error, a compensation method with the amplitude control in the DOC direction has been proposed by applying EVC. The dynamic motion error of the liner motion axis has been detected by utilizing a highly-precise liner encoder built in the machine tool. Furthermore, the motion error is converted into a voltage command in real time for achieving the amplitude control, thus, guaranteeing that the vibration amplitude variation precisely auto-tracks the dynamic position of the motion axis in the DOC direction for maintaining a constant nominal DOC value. In order to analyze the machining performance of the proposed compensation method, a series of analytical and experimental investigations have been conducted during the planing process. The maximum contour error is noted to effectively decrease from ~0.6 to 0.04 μm by applying the proposed compensation method for flat surface machining. Finally, the micro-dimple array with a structural height from 0.2 to 0.6 μm has fabricated on the hardened steel with a maximum contour error of less than 0.04 μm, which verifies the feasibility of the proposed amplitude control compensation method. The proposed contour error compensation method also makes the machining process

more precise, efficient and smart.

Acknowledgments

Authors acknowledge Taga Electric Co., Ltd. and Nachi-Fujikoshi Co., Ltd. for their experimental support. Jianguo Zhang is grateful for the part of original support from the National Natural Science Foundation of China (No. 51905194) and the Wuhan Science and Technology Plan in China (No. 2019010701011400).

References

[1] Zhou XT, Weng YL, Peng YY, Chen GX, Lin JP, Yan Q, Zhang YA, Guo TL. Design and fabrication of square micro-lens array for integral imaging 3D display. Optik 2018; 157: 532-539.

[2] http://cpn.canon-europe.com/content/education/technical/eos_70d_technology.do

[3] Fang FZ, Zhang XD, Weckenmann A, Zhang GX, Evans C. Manufacturing and measurement of freeform optics. CIRP Annals-Manufacturing Technology 2013; 62(2): 823-846.

[4] Brinksmeier E, Riemer O, Gläbe R, Lünemann B, Kopylow C, Dankwart C, Meier A. Submicron functional surfaces generated by diamond machining. CIRP Annals-Manufacturing Technology 2010; 59: 535-538.

[5] Brinksmeier E, Glabe R, Schonemann L. Review on diamond-machining processes for the generation of functional surface structures. CIRP Journal of Manufacturing Science and Technology 2012; 5: 1-7.

[6] Yan JW, Oowada T, Zhou TF, Kuriyagawa T. Precision machining of microstructures on electroless-plated NiP surface for molding glass components. Journal of Materials Processing Technology 2009; 209: 4802-4808.

[7] Paul E, Evans CJ, Mangamelli A, McGlauflin ML, Polvani RS. Chemical aspects of tool wear in single point diamond turning. Precision Engineering 1996; 18(1): 4-19.

[8] Shamoto E, Moriwaki T. Study on elliptical vibration cutting. CIRP Annals-Manufacturing Technology 1994; 43(1): 35-38.

[9] Shamoto E, Moriwaki T. Ultaprecision diamond cutting of hardened steel by applying

elliptical vibration cutting. CIRP Annals-Manufacturing Technology 1999; 48(1): 441-444.

[10] Suzuki N, Nakamura A, Shamoto E, Harada K, Matsuo M, Osada M. Ultraprecision micromachining of hardened steel by applying ultrasonic elliptical vibration cutting. Proceedings of International Symposium on Micromechatronics and Human Science 2003; Nagoya, Japan, 221-226.

[11] Guo J, Zhang JG, Pan YN, Kang RK, Namba Y, Shore P, Yue XB, Wang BR, Guo DM. A critical review on the chemical wear and wear suppression of diamond tools in diamond cutting of ferrous metals. International Journal of Extreme Manufacturing 2020; 2: 012001.

[12] Zhang XQ, Kumar AS, Rahman M, Nath C, Liu K. Experimental study on ultrasonic elliptical vibration cutting of hardened steel using PCD tools. Journal of Materials Processing Technology 2011; 211: 1701-1709.

[13] Suzuki N, Yokoi H, Shamoto E. Micro/nano sculpturing of hardened steel by controlling vibration amplitude in elliptical vibration cutting. Precision Engineering 2011; 35: 44-50.

[14] Zhang JG, Suzuki N, Wang YL, Shamoto E. Ultra-precision nano-structure fabrication by amplitude control sculpturing method in elliptical vibration cutting. Precision Engineering 2015; 39: 86-99.

[15] Zhang JG, Cui T, Ge C, Sui YX, Yang HJ. Review of micro/nano machining by utilizing elliptical vibration cutting. International Journal of Machine Tools and Manufacture 2016; 106: 109-126.

[16] Moon JH, Lee BG. Modeling and sensitivity analysis of a pneumatic vibration isolation system with two air chambers. Mechanism and Machine Theory 2010; 45: 1828-1850.

[17] Lee J, Okwudire CE. Reduction of vibrations of passively-isolated ultra-precisionmanufacturing machines using mode coupling. Precision Engineering 2016; 43: 164-177.

[18] Sencer B, Ishizaki K, Shamoto E. High speed cornering strategy with confined contour error and vibration suppression for CNC machine tools. CIRP Annals -

Manufacturing Technology 2015; 64: 369-372.

[19] Tajima S, Sencer B, Shamoto E. Accurate interpolation of machining tool-paths based on FIR filtering. Precision Engineering 2018; 52: 332-344.

[20] Altintas Y, Verl A, Brecher C, Uriarte L, Pritschow G. Machine tool feed drives. CIRP Annals - Manufacturing Technology 2011; 60(2): 779-796.

[21] Altintas Y, Khoshdarregi MR. Contour error control of CNC machine tools with vibration avoidance. CIRP Annals - Manufacturing Technology 2012; 61: 335-338.

[22] Hosseinabadi AH, Altintas Y. Modeling and active damping of structural vibrations in machine tools. CIRP Journal of Manufacturing Science and Technology 2014; 7: 246-257

[23] Dumanli A, Sencer B. Optimal high-bandwidth control of ball-screw drives with acceleration and jerk feedback. Precision Engineering 2018; 54: 254-268.

[24] Zhu WH, Jun MB, Altintas Y. A fast tool servo design for precision turning of shafts on conventional CNC lathes. International Journal of Machine Tools and Manufacture 2001; 41: 953-965.

[25] Gao W, Tano M, Araki T, Kiyono S, Park CH. Measurement and compensation of error motions of a diamond turning machine. Precision Engineering 2007; 31: 310-316.

[26] Kim HS, Kim EJ. Feed-forward control of fast tool servo for real-time correction of spindle error in diamond turning of flat surfaces. International Journal of Machine Tools and Manufacture 2003; 43: 1177-1183.

[27] Fujishima M, Ohno K, Nishikawa S, Nishimura K, Sakamoto M, Kawai K. Study of sensing technologies for machine tools. CIRP Journal of Manufacturing Science and Technology 2016; 14: 71-75.

[28] Golubovic E, A. Baran E, Sabanovic A. Contouring Controller for Precise Motion Control Systems. Automatika 2013; 54: 19-27.